Tunable Center Frequency Negative Group Delay Filter Using Coupling Matrix Approach

Girdhari Chaudhary, *Member, IEEE*, and Yongchae Jeong, *Senior Member, IEEE*

***Abstract*— In this letter, a negative group delay filter (NGDF) with tunable center frequencies is presented. The proposed filter is designed using finite unloaded-Q_u resonators based on the coupling matrix approach. The proposed NGDF does not require a lumped resistor to generate a negative group delay and has source-load and inter-resonator couplings. The center frequency of the filter is tuned by varying the bias voltage of the varactor diodes. The design theory for the proposed filter is validated experimentally through fabrication of a second-order NGDF at a center frequency of 2.14 GHz.**

***Index Terms*— Coupling matrix, finite unloaded-quality factor, negative group delay, tunable center frequency.**

I. INTRODUCTION

TUNABLE filter design is an active research topic today. Therefore, several tunable filters with tunable center frequency, bandwidth control, enhanced stop band performances or a wide tuning range, and bandstop to bandpass switchable filters have been presented in the literature. However, group delay (GD) analysis of these filters has not been performed [1].

Negative group delay (NGD) refers to the phenomenon whereby an electromagnetic wave traverses a dispersive material or electronic circuit in such a manner that its amplitude envelope is advanced through media without a delay [2]. However, this phenomenon does not violate the principle of causality. The conventional approaches to realize NGD circuits are based on *RLC* resonators, which suffer from high signal attenuation (SA), smaller NGD bandwidth, magnitude (S_{21}) flatness, and fixed center frequency [3]. While a few studies have been performed on reducing SA [4]–[6], these works still suffer from small NGD bandwidth and the magnitude flatness problem. To overcome these problems, researchers have attempted to design NGD circuits using different methods such as cross-coupling between resonators [7], increasing the number of resonators [8] and transversal-filter topologies [9]. On the other hand, these works showed very high SA ($>$28 dB for -1 ns). Except for the work in [9], these NGD circuits also used resistor R for generating NGD, which prevents fully distributed circuit realization.

In this letter, a fully distributed negative group delay filter (NGDF) with tunable center frequencies is presented. The design method is based on a coupling matrix along with finite unloaded-quality factor (Q_u) resonators. This proposed NGDF does not require any R for generating NGD, or any extra network for matching input/output ports with reference termination impedances.

Manuscript received June 22, 2016; accepted August 9, 2016. Date of publication December 12, 2016; date of current version January 6, 2017. This work was supported by the Basic Science Research Program through the National Research Foundation of Korea (NRF) funded by the Ministry of Education, Science and Technology (2016R1D1A1A09918818).

The authors are with the Division of Electronics and Information Engineering, IT Research Center, Chonbuk National University, Jollabuk-do 54896, Republic of Korea (e-mail: ycjeong@jbnu.ac.kr).

Color versions of one or more of the figures in this paper are available online at http://ieeexplore.ieee.org.

Digital Object Identifier 10.1109/LMWC.2016.2629985

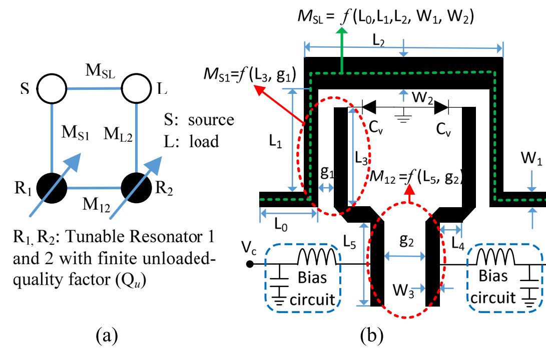

Fig. 1. Proposed structure of tunable negative group delay filter: (a) coupling diagram and (b) simulation layout with physical dimensions. Physical dimensions: $L_0 = 13.8$, $L_1 = 10.2$, $L_2 = 22.4$, $L_3 = 9.6$, $L_4 = 1.5$, $L_5 = 17$, $W_1 = W_3 = 1.8$, $W_2 = 3.5$, $g_1 = 0.8$, and $g_2 = 7$. (Unit: mm).

II. THEORY AND DESIGN EQUATIONS

Fig. 1 shows the coupling diagram for the proposed second-order NGDF where both external couplings (M_{S1} and M_{L2}) are equal. Similarly, the resonator self-coupling values (M_{11} and M_{22}), the source-to-load (M_{SL}) coupling, and the load-to-source coupling (M_{LS}) have the same magnitude. With a finite unloaded quality factor Q_u of resonators, the $(N+2) \times (N+2)$ coupling matrix of the generalized second-order filter [1] corresponding to the coupling diagram shown in Fig. 1 is given as (1).

$$M = \begin{bmatrix} 0 & M_{S1} & 0 & M_{SL} \\ M_{S1} & M_{11}+x & M_{12} & 0 \\ 0 & M_{12} & M_{22}+x & M_{S1} \\ M_{SL} & 0 & M_{S1} & 0 \end{bmatrix} \quad (1)$$

where the subscripts S, L, 1, and 2 correspond to the source, load, the first resonator and the second resonator, respectively.

Furthermore, assuming lossless coupling between source and load (M_{SL}) and $M_{11} = M_{22} = -j/Q_u\Delta$, the reflection ($S_{11}$) and transmission ($S_{21}$) responses corresponding to the coupling relationship (1) are given as (2), where Q_u and Δ are unloaded quality factor and 1-dB fractional bandwidth of resonators [1] which is defined as $\Delta = (f_2 - f_1)/f_0$. Here, f_2 and f_1 are 1-dB frequencies above the maximum insertion loss at center frequency (f_0), which are given by (2a)–(2c) shown at the bottom of the next page where, ω and ω_0 are the operating and center angular frequencies of NGDF. For matched input/output ports, S_{11} in (2a) is set to zero at $\omega = \omega_0$ in order to find the relationship between M_{SL} and M_{S1} with the assumption of $x = 0$, and $M_{12} = aM_{S1}^2$, where a is any real positive value. For an arbitrary value of M_{S1}, the relationship between M_{SL} and M_{S1} for matched input/output ports at $\omega = \omega_0$ can be found with (3).

Furthermore, using (2b), the GD of the proposed NGDF can be calculated as (4), where M_{SL} can be obtained from (3) for

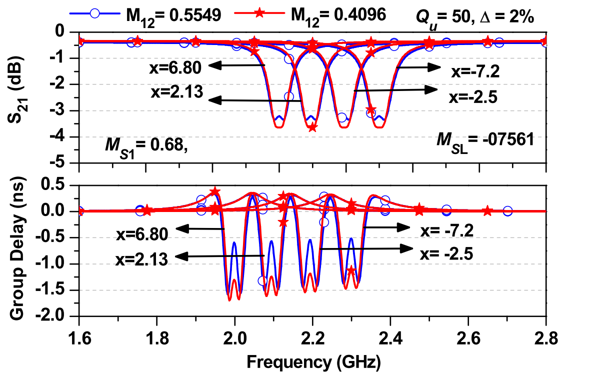

Fig. 2. Calculated magnitude/group delay responses for the proposed NGDF.

the matched input/output condition at center frequency f_0.

$$\tau_g = -\frac{\omega^2+\omega_0^2}{\omega_0\omega^2\Delta}\frac{d\angle S_{21}}{d\Omega} \tag{4}$$

To illustrate the above design equations, the synthesized responses of the proposed NGDF are shown in Fig. 2. As observed, the center frequency is tuned from 2 to 2.3 GHz by controlling the tuning element value from 6.8 to -7.2. Similarly, S_{21} is increased as M_{12} increases toward a higher value. Moreover, the maximum GD and the NGD bandwidth (which is defined as bandwidth when GD < 0) are also increased when M_{12} changes from 0.4096 to 0.5549, indicating the need to control the coupling between resonators 1 and 2.

In these simulations, input and output return losses are higher than -60 dB at tunable center frequencies. Since input/output ports are matched while center frequency is tuned, the circuit does not need any extra matching circuits.

III. Implementation and Experimental Performances

The physical implementation of the proposed NGDF can be summarized as follows:

(a) Firstly, specify the tunability frequency range, maximum achievable GD, magnitude of S_{21}, Q_u, and Δ.

(b) Calculate M_{SL} using (2) by providing value of M_{S1} and a.

(c) Calculate GD, S_{21} and compare with specified values. If the calculated GD and S_{21} are almost similar with the specified, the coupling matrix concurs with specification of filter.

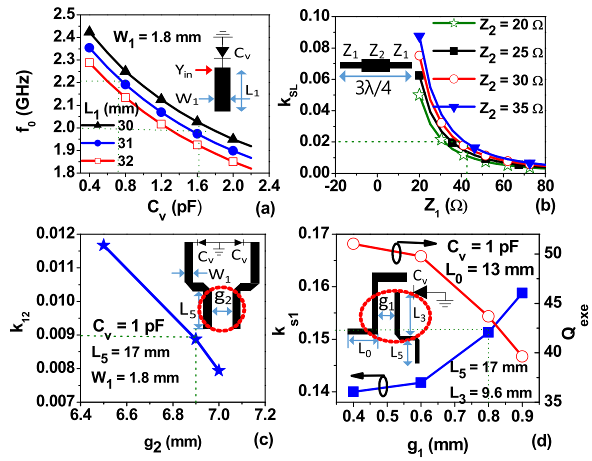

Fig. 3. Extracted parameters with FR4-epoxy substrate with $\varepsilon_r = 4.4$, $h = 0.787$ mm, and $\tan\delta = 0.02$: (a) resonant frequencies with variation of C_v, (b) source-load coupling coefficient k_{sL}, (c) inter-resonator coupling coefficient k_{12}, and (d) input/output coupling coefficients (k_{s1} and Q_{exe}).

(d) Estimate the range of capacitance, length, and width of transmission line based on frequency tunability range. For illustration, the resonant frequency variation with length of transmission line and capacitance C_v are plotted in Fig. 3(a).

(e) After obtaining normalized coupling matrix, calculate coupling coefficient k_{s1}, k_{12}, and k_{SL} using

$$k_{S1} = M_{S1}\sqrt{\Delta} = 1/\sqrt{Q_{exe}}, \quad k_{12} = M_{12}\Delta, \quad k_{SL} = M_{SL}\Delta. \tag{5}$$

(f) Implement k_{sL} with $3\lambda/4$ step impedance line with characteristic impedance of Z_1 and Z_2. The relation between characteristic impedances and k_{sL} is given as (6). The extracted k_{sL} is show in Fig. 3(b).

$$k_{SL} = \frac{Z_2}{Z_1^2} \tag{6}$$

(g) The inter-resonator coupling coefficient k_{12} can be extracted by controlling length L_5 and gap g_2 as shown in Fig. 3(c). Similarly, k_{s1} can be extracted by controlling L_3 and g_1 as shown in Fig. 3(d).

(h) Finally optimized overall circuit using EM simulator.

For experimental demonstration purposes, a second-order NGDF was fabricated with f_0 of 2.14 GHz on an FR-4 epoxy

$$S_{11} = 1 - \frac{\Omega^2 + \left(x - \frac{j}{Q_u\Delta}\right)^2 + \left(x - \frac{j}{Q_u\Delta}\right)\left(2\Omega - jM_{S1}^2\right) - M_{12}^2 - jM_{S1}^2\Omega}{\left[\begin{array}{l} 0.5\left(M_{SL}^2+1\right)\left\{\left(x - \frac{j}{Q_u\Delta}\right)^2 - M_{12}^2 + \Omega^2\right\} + \left(x - \frac{j}{Q_u\Delta}\right)\left(\Omega + M_{SL}^2\Omega - jM_{S1}^2\right) \\ +M_{12}M_{S1}^2M_{SL} - 0.5M_{S1}^4 - jM_{S1}^2\Omega \end{array}\right]} \tag{2a}$$

$$S_{21} = \frac{2\left\{M_{SL}\left(\Omega^2 + \left(x - \frac{j}{Q_u\Delta}\right)^2 + 2\left(x - \frac{j}{Q_u\Delta}\right)\Omega\right) - M_{SL}M_{12}^2 + M_{12}M_{S1}^2\right\}}{\left[\begin{array}{l} 2\left(x - \frac{j}{Q_u\Delta}\right)\left(M_{S1}^2 + jM_{SL}^2\Omega + j\Omega\right) + j\left(M_{SL}^2+1\right)\left\{\Omega^2 + \left(x - \frac{j}{Q_u\Delta}\right)^2 - M_{12}^2\right\} \\ +2jM_{12}M_{S1}^2M_{SL} - jM_{S1}^4 + 2M_{S1}^2\Omega \end{array}\right]} \tag{2b}$$

$$\Omega = \frac{1}{\Delta}\left(\frac{\omega}{\omega_0} - \frac{\omega_0}{\omega}\right) \tag{2c}$$

$$M_{SL} = \frac{aM_{S1}^4 \mp \sqrt{a^2M_{S1}^8 + \left(a^2M_{S1}^4 + \frac{1}{Q_u^2\Delta^2}\right)\left\{M_{S1}^4\left(a^2-1\right) + \frac{1}{Q_u^2\Delta^2}\right\}}}{a^2M_{S1}^4 + \frac{1}{Q_u^2\Delta^2}} \tag{3}$$

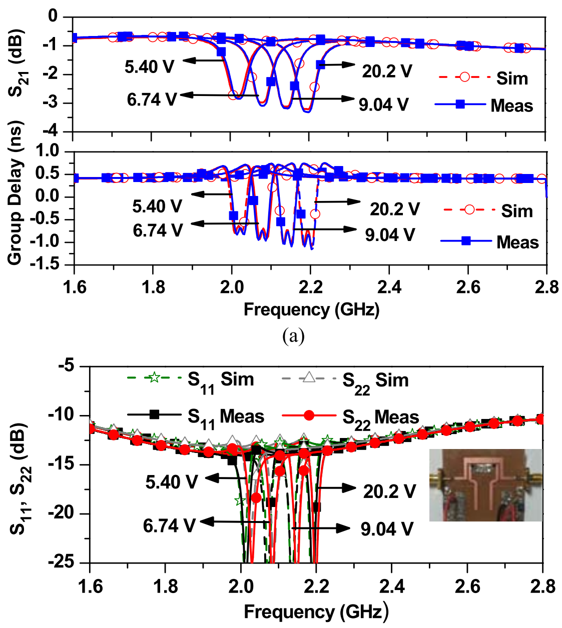

Fig. 4. Simulated and measured results for the proposed negative group delay filter: (a) magnitude/group delay and (b) return losses.

substrate with dielectric constant (ε_r) of 4.4, thickness (h) of 0.787 mm, and loss tangent of 0.02. The goal of the design filter was to achieve a GD of -1 ns with insertion loss of less than 4 dB and center frequency tunability of 2 to 2.2 GHz under the assumption of a termination port impedance Z_0 of 50 Ω. As described above, the coupling matrix was extracted for the given specification of the filter as $M_{S1} = 1.1$, $M_{12} = 1.2705$, $M_{SL} = 1.4745$ with $Q_u = 50$ and $\Delta = 2\%$. In addition, the calculated coupling coefficients are given as $Q_{exe} = 41.32$, $k_{s1} = 0.156$, $k_{12} = 0.009$ and $k_{sL} = 0.02$. The simulation was performed using ANYSYS HFSS 15.

The resonators were implemented with an open-circuited $\lambda/2$ transmission line with terminated with varacator diode as shown in Fig. 1(b). Using HFSS Eigen-mode simulation, the Q_u of the $\lambda/2$ resonator in the FR-4 epoxy substrate is estimated to be around 50. Similarly, the coupling between the source and load was implemented with a step-impedance $3\lambda/4$ line. Based on the extracted coupling coefficients and EM simulation optimization, the physical dimensions of the implemented filter are shown in Fig. 1(b). The bias line was implemented using $\lambda/4$ line at f_0 with high characteristic impedance. In this work, the tuning element was implemented using SMV 1233-011LF varactor diodes from Skyworks Inc. The photograph of the fabricated second-order filter is shown in Fig. 4(b).

The simulated and measured results are shown in Fig. 4. The measurement results are in good agreement with the simulations. From the measurement results shown in Fig. 4(a), the center frequency was tuned from 2.02 to 2.20 GHz by varying the bias voltage of the varactor diodes from 5.40 to 20.2 V. The measured insertion loss and GD variations were determined to be -2.92 to -3.25 dB and -0.77 ± 0.11 ns to -0.87 ± 0.05 ns, respectively. The NGD bandwidth was 60 MHz, providing the NGD-bandwidth product of 0.0468. Similarly, the measured input/output return losses were higher than 18.88 dB at each center frequencies as shown in Fig. 4(b). Moreover, the return loss was higher than 12 dB in the frequency range of 100 MHz. The performance of the proposed NGDF is compared with previous studies and shown in Table I.

TABLE I

PERFORMANCE COMPARISON

	f_0 (GHz	SA_{max} (dB)	GD_{max} (ns)	FT	FOM
[3]	1.0	-32.50	-10.0	N	0.022
[4]	2.14	-16.90	-7.90	N	0.019
[5]	2.14	-17.45	-7.48	N	0.023
[6]	2.14	-15.38	-6.48	N	0.024
[7]	1.962	-29.30	-1.10	N	0.021
[9]	1.0	-38.50	-1.50	N	0.026
This work	**2.02 to 2.20**	**-2.92 to -3.25**	**-0.77±0.10/ -0.87±0.05**	**Y**	**0.027/ 0.029**

SA_{max} : Maximum signal attenuation at f_0, FT: Frequency tunability

In the NGD circuit, the SA can be interpreted as an out-of-band gain as compared to NGD band. Therefore, the SA should be small as possible. In addition, it can observed that larger NGD and bandwidth can be achieved by accepting increased amount of SA.

Due to the trade-off between the maximum achieved GD, the maximum SA, and the NGD bandwidth, the figure of merit (FOM) of NGD circuits can be defined as

$$\text{FOM} = -\frac{GD_{\max}|_{f=f_0} \times NGD\_BW}{\sqrt{|\text{SA}_{\max,\text{dB}}|}}. \tag{7}$$

As seen in Table I, the proposed NGDF provides frequency tunability, the highest FOM and the best performance in terms of GD/magnitude flatness and SA.

IV. CONCLUSION

In this letter, we demonstrated the design of a negative group delay filter with tunable center frequencies and predefined negative group delay. The filter was designed by using the coupling matrix filter synthesis approach, which does not require any resistors to generate negative group delay. The proposed filter provides wide magnitude flatness and negative group delay bandwidth, which can be controlled by inter-resonator couplings. The input/output ports are matched at each center frequencies without an additional matching network. The signal attenuation of proposed filter is also small compare to conventional negative group delay circuits.

REFERENCES

[1] E. J. Naglich, J. Lee, D. Peroulis, and W. J. Chappell, "Switchless tunable bandstop-to-all-pass reconfigurable filter," *IEEE Trans. Microw. Theory Techn.*, vol. 60, no. 5, pp. 1258–1265, May 2012.

[2] C. H. Hymel, M. H. Skolnick, R. A. Stubbers, and M. E. Brandt, "Temporally advanced signal detection: A review of the technology and potential applications," *IEEE Circuits Syst. Mag.*, vol. 11, no. 3, pp. 10–25, 3rd Quart., 2011.

[3] S. Lucyszyn, I. D. Robertson, and A. H. Aghvami, "Negative group delay synthesizer," *Electron. Lett.*, vol. 29, no. 9, pp. 798–800, Apr. 1993.

[4] G. Chaudhary and Y. Jeong, "Distributed transmission line negative group delay circuit with improved signal attenuation," *IEEE Microw. Wireless Compon. Lett.*, vol. 24, no. 1, pp. 20–22, Jan. 2014.

[5] G. Chaudhary and Y. Jeong, "Transmission-line negative group delay networks with improved signal attenuation," *IEEE Antennas Wireless Propag. Lett.*, vol. 13, pp. 1039–1042, 2014.

[6] G. Chaudhary and Y. Jeong, "Low signal-attenuation negative group-delay network topologies using coupled lines," *IEEE Trans. Microw. Theory Techn.*, vol. 62, no. 10, pp. 2316–2324, Oct. 2014.

[7] G. Chaudhary and Y. Jeong, "A design of compact wideband negative group delay network using cross coupling," *Microw. Opt. Technol. Lett.*, vol. 56, no. 11, pp. 2612–2616, Nov. 2014.

[8] G. Chaudhary, Y. Jeong, and J. Lim, "Microstrip line negative group delay filters for microwave circuits," *IEEE Trans. Microw. Theory Techn.*, vol. 62, no. 2, pp. 234–243, Feb. 2014.

[9] C. T. Michael and T. Itoh, "Maximally flat negative group delay circuit: A microwave transversal filter approach," *IEEE Trans. Microw. Theory Techn.*, vol. 62, no. 6, pp. 1330–1342, Jun. 2014.